Multiparameter control of chaos

Ernest Barreto
Department of Physics and Institute for Plasma Research, University of Maryland, College Park, Maryland 20742

Celso Grebogi
Department of Mathematics, Institute for Plasma Research, and Institute for Physical Science and Technology, University of Maryland, College Park, Maryland 20742

(Received 3 April 1995)

Controlling chaos by using more than one available control parameter is presented as an experimentally feasible way to reduce the transient times that precede stabilization and improve performance in the presence of noise. We demonstrate these advantages by applying our method to a numerical example.

PACS number(s): 05.45.+b

Recently, a great deal of attention has been focused on the idea that small adjustments to an available system parameter can be used to stabilize unstable periodic orbits in chaotic systems [1,2]. Numerous experiments in many diverse fields have demonstrated the feasibility of this approach. For example, this technique has been applied to mechanical systems [3], lasers [4], circuits [5], chemical reactions [6], biological systems [7], etc. Furthermore, it is possible to switch from one periodic orbit to another at will [2,3,8]. In all the references cited above, control is achieved by judiciously adjusting only a single available control parameter, even though, in principle, several such parameters are available for use.

The method of Refs. [1,2] assumes that the control perturbations are limited to be small, and hence is based on a linearization of the dynamics in the immediate vicinity of the orbit that is to be stabilized. Thus, one must wait for the chaotic trajectory to approach this small region before applying the stabilization procedure. In the case of even moderately high-dimensional systems, these chaotic transient times can be prohibitively long. Several targeting methods have been proposed to deal with this problem [8,9]; however, these methods require extensive knowledge of the dynamics, which often is not available in an experimental situation.

In this paper, we extend the method of Refs. [1,2] to allow for the simultaneous use of several control parameters. Warncke *et al.* have considered this problem in the context of controlling very high-dimensional chaotic systems [10]; here we adopt the well-known pole placement formalism and demonstrate that multiparameter control constitutes an experimentally feasible way to significantly reduce the chaotic transient times. Furthermore, we show that the resulting stabilization is more effective and resilient in the presence of noise.

To illustrate our results, we compare one and two parameter control as applied to the kicked double rotor (see Fig. 1). This is a system of two connected rods subjected to periodic impulsive kicks. The time evolution, sampled immediately after each kick, is given by a four-dimensional map [2,11]. We take our control parameters to be the strength of the kick ρ and the angle ϕ at which the kick is applied. Small perturbations $|\delta\rho| \leq \rho_*$ and/or $|\delta\phi| \leq \phi_*$ are applied around nominal values ($\rho_0 = 9.0, \phi_0 = 0.0$) at which the map exhibits 36 fixed points within a chaotic attractor of Lyapunov dimension 2.8 (see figure caption for further details).

For simplicity, we consider the stabilization of a fixed point $\mathbf{x}_f$, that is, an unstable periodic orbit of period one. A chaotic trajectory beginning at a random initial condition on the attractor can be stabilized at $\mathbf{x}_f$ after a transient time t, where t has a distribution of the form

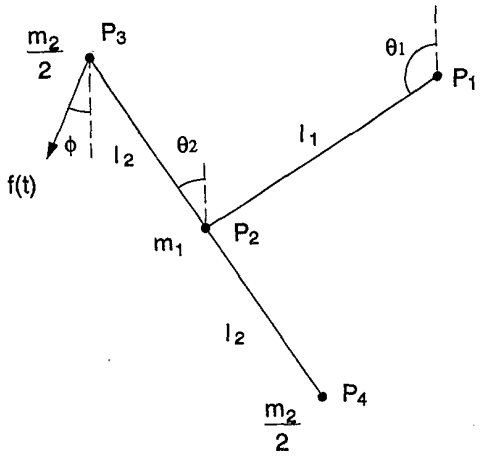

FIG. 1. The kicked double rotor. A massless rod of length l_1 pivots about the stationary point P_1. A second massless rod of length $2l_2$ is mounted on pivot P_2, which in turn is mounted at the end of the first rod. Periodic impulsive kicks $f(t) = \sum_{n=0}^{\infty} \rho_n \delta(t-n)$ are applied at an angle ϕ as shown. The state of the system immediately after the $(n+1)$th kick is given by a four-dimensional map of the form $\mathbf{X}_{n+1} = \mathbf{M}\mathbf{Y}_n + \mathbf{X}_n$ and $\mathbf{Y}_{n+1} = \mathbf{L}\mathbf{Y}_n + \mathbf{G}(\mathbf{X}_{n+1})$, where $\mathbf{X} = (\theta_1, \theta_2)^T$ are the two angular position coordinates, $\mathbf{Y} = (\dot{\theta}_1, \dot{\theta}_2)^T$ are the corresponding angular velocities, and $\mathbf{G}(\mathbf{X})$ is a nonlinear function. $\mathbf{M}$ and $\mathbf{L}$ are both constant matrices, which involve the coefficients of friction at the two pivots and the moments of inertia of the rotor. Gravity is absent. Control parameters at time n are $\rho_n = 9.0 + \delta\rho_n$ and $\phi_n = 0.0 + \delta\phi_n$. We take $l_2 = 1/\sqrt{2}$, and set all other parameters to 1. For further details, see Refs. [2,11].

$\exp(-t/\langle t\rangle)$ for large t. Here $\langle t\rangle$ depends on the size of the region around $\mathbf{x}_f$ in which the control procedure can be successfully applied, and hence depends on (i) the maximum permitted parameter perturbations ρ_* and/or ϕ_*, and (ii) the extent to which the linearization used to calculate the perturbations accurately reflects the dynamics in this region [1].

In order to meaningfully compare the transient times for one versus two parameter control, we proceed as follows. First, we select a value of ρ_* and use one parameter ρ control to measure the resulting $\langle t\rangle$. We then find a value for ϕ_* such that one parameter ϕ control yields the *same* value for $\langle t\rangle$. This time can then be compared to the time resulting from controlling using both parameters, subject to the restrictions $|\delta\rho| \le \rho_*$ and $|\delta\phi| \le \phi_*$.

We use two different fixed points, one with one unstable direction, and the other with two unstable directions. The results are presented in Fig. 2. For purposes of visual comparison, we plot $\langle t\rangle$ for one and two parameter control versus ϕ_*. The multiparameter case is seen to show a reduction of up to an order of magnitude in the transient time. We emphasize that this improvement has been obtained only by assuming that an additional control parameter is available for use. This is often the case in experimental situations.

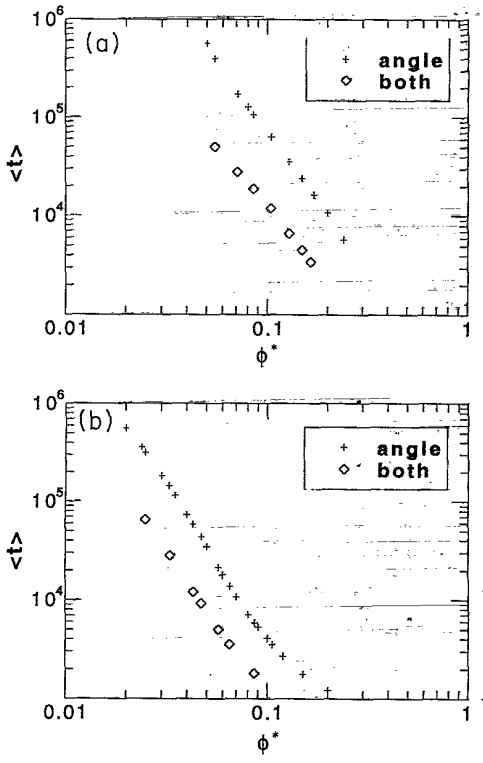

FIG. 2. The transient times $\langle t\rangle$ vs ϕ^* for one parameter (+) and two parameter ($\diamond$) control for (a) a fixed point with two unstable directions, and (b) a fixed point with one unstable direction. The one parameter results are obtained by applying small perturbations to ϕ subject to the restriction $|\delta\phi| \le \phi^*$. The two parameter results are similarly obtained under the restrictions $|\delta\phi| \le \phi^*$ and $|\rho| \le \rho^*$, where ϕ^* and ρ^* are chosen as described in the text. The two parameter results show an improvement of up to an order of magnitude in the transient times.

We next consider the effect of noise on stabilized orbits. If the noise amplitude is large enough, control can be temporarily lost, and the orbit returns to the attractor at large. To model this effect, we stabilize a fixed point, then add random perturbations of increasing amplitude to each component of the state at each iterate. (More specifically, we use random numbers drawn from a uniform distribution on the interval $[-A, A]$, where A is the noise amplitude.) We measure how much noise a stabilized fixed point can tolerate by making 1000 attempts to hold an orbit for 1000 iterations at each noise level. Figure 3 shows a plot of the average number of iterations for which the fixed point remained stabilized versus noise amplitude. The two cases of one parameter control were seen to fail at significantly lower noise amplitudes than the multiparameter control case.

If the noise is small, a controlled orbit occupies a small cloud in the vicinity of the fixed point. A typical distribution of distances from the fixed point is shown in Fig. 4. We find that multiparameter control is more effective in the sense that it leads to a distribution that is narrower and peaked at a smaller distance than in the two cases of one parameter control. This was observed at all noise amplitudes at which the fixed point in question could be stabilized.

We now describe the stabilization formalism for multiparameter control. Suppose we have a system whose dynamics is governed by a d-dimensional map $\mathbf{x}_{n+1} = \mathbf{F}(\mathbf{x}_n, \mathbf{p}_n)$, where $\mathbf{p}_n$ is a vector of r available control parameters. We would like to stabilize a fixed point

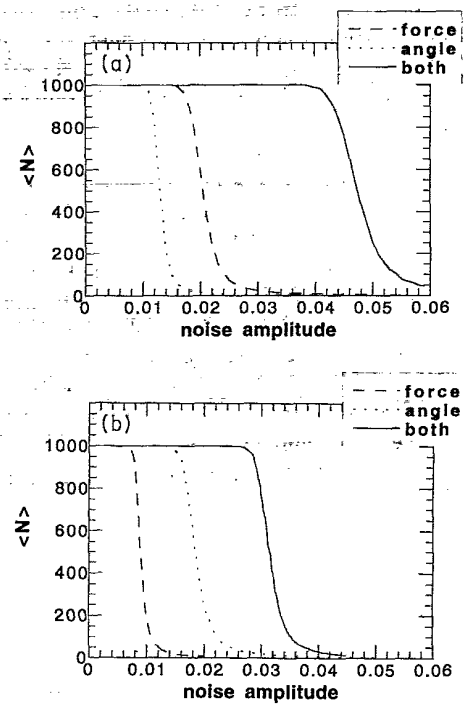

FIG. 3. The average number $\langle N\rangle$ of iterations (maximum 1000) for which a fixed point remains stabilized vs noise amplitude, for the same fixed points as in Fig. 2. Two parameter control is seen to tolerate larger noise amplitudes.

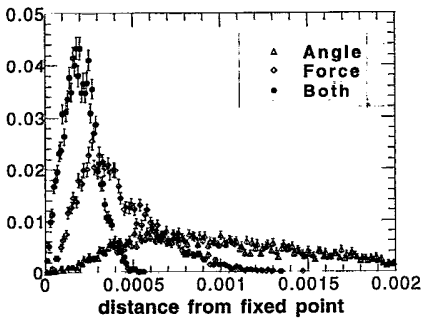

FIG. 4. The distribution of distances of a controlled orbit from the fixed point about which it is stabilized, in the presence of noise, for a typical (ρ^*, ϕ^*) pair (see text). Here the noise amplitude is 0.001; similar distributions were observed at all amplitudes at which the fixed point could be stabilized. The multiparameter distribution is narrower and peaked at a smaller distance than the one parameter cases.

$\mathbf{x}^*$ (which exists for the parameter values $\mathbf{p}_0$) by making small perturbations $\delta p^{(1)}, \ldots, \delta p^{(r)}$ to the r parameters subject to the restrictions $|\delta p^{(1)}| \leq p_*^{(1)}, |\delta p^{(2)}| \leq p_*^{(2)}, \ldots, |\delta p^{(r)}| \leq p_*^{(r)}$. Without loss of generality, let us replace $(\mathbf{x}_n - \mathbf{x}^*)$ by $\mathbf{x}_n$, and $(\mathbf{p}_n - \mathbf{p}_0)$ by $\mathbf{p}_n$. We approximate the dynamics in the vicinity of $\mathbf{x} = \mathbf{0}$ by

$$\mathbf{x}_{n+1} = \mathbf{A}\mathbf{x}_n + \mathbf{B}\mathbf{p}_n, \tag{1}$$

where $\mathbf{A} = \frac{\partial \mathbf{F}}{\partial \mathbf{x}}|_{\mathbf{x}=\mathbf{0}}$ is a $(d \times d)$ matrix and $\mathbf{B} = \frac{\partial \mathbf{F}}{\partial \mathbf{p}}|_{\mathbf{p}=\mathbf{0}}$ is a $(d \times r)$ matrix. Then writing $\mathbf{p}_n = -\mathbf{K}\mathbf{x}_n$, where $\mathbf{K}$ is a $(r \times d)$ matrix, we have $\mathbf{x}_{n+1} = (\mathbf{A} - \mathbf{B}\mathbf{K})\mathbf{x}_n$. For a *controllable* system, standard techniques (i.e., pole placement) allow us to find the matrix $\mathbf{K}$ such that $(\mathbf{A} - \mathbf{B}\mathbf{K})$ has any desired eigenvalues. (The controllability condition and the construction of $\mathbf{K}$ are described in the Appendix; see also Ref. [12].) By selecting eigenvalues of magnitude less than one, $\mathbf{x}_n$ approaches $\mathbf{0}$.

If $\mathbf{x}$ is large, the above linearization cannot be expected to be valid. Hence, we calculate the control perturbations at every iteration, and if the prescribed values are not within the allowed ranges, we proceed at the unperturbed parameter values. When using several control parameters, the calculated perturbations may be in range for only a few of the components of $\mathbf{p}$. In our numerical example, we only apply the perturbations if all calculated values are within the allowed ranges. See below for a discussion of other possibilities. This process is repeated until 100 consecutive iterations yield perturbations within the allowed ranges; we take this to be our definition of achieving control.

A matrix $\mathbf{T}$ can be constructed (see the Appendix) that transforms Eq. (1) to the controllable canonical form $\hat{\mathbf{x}}_{n+1} = \tilde{\mathbf{A}}\hat{\mathbf{x}}_n + \tilde{\mathbf{B}}\mathbf{p}$, where $\mathbf{x}_n = \mathbf{T}\hat{\mathbf{x}}_n$, $\tilde{\mathbf{A}} = \mathbf{T}^{-1}\mathbf{A}\mathbf{T}$, $\tilde{\mathbf{B}} = \mathbf{T}^{-1}\mathbf{B}$, and $\tilde{\mathbf{K}} = \mathbf{K}\mathbf{T}$. For computational convenience, we have chosen $\mathbf{K}$ in our numerical example such that $(\mathbf{A} - \mathbf{B}\mathbf{K})$ has zero eigenvalues. Thus, $(\tilde{\mathbf{A}} - \tilde{\mathbf{B}}\tilde{\mathbf{K}})$ will also have zero eigenvalues, and in particular, will be a block nilpotent matrix with zeros along the diagonal. This contruction therefore collapses the state vector onto the fixed point in a minimum number of steps n_{min} equal to the dimension of the largest nilpotent block in $(\tilde{\mathbf{A}} - \tilde{\mathbf{B}}\tilde{\mathbf{K}})$. For example, in a four-dimensional system with one control parameter, $\mathbf{K}$ can be constructed such that

$$(\tilde{\mathbf{A}} - \tilde{\mathbf{B}}\tilde{\mathbf{K}}) = \begin{pmatrix} 0 & 1 & 0 & 0 \\ 0 & 0 & 1 & 0 \\ 0 & 0 & 0 & 1 \\ 0 & 0 & 0 & 0 \end{pmatrix}.$$

This will lead a succession of state vectors

$$\hat{\mathbf{x}} = \begin{pmatrix} x_1 \\ x_2 \\ x_3 \\ x_4 \end{pmatrix} \rightarrow \begin{pmatrix} x_2 \\ x_3 \\ x_4 \\ 0 \end{pmatrix} \rightarrow \begin{pmatrix} x_3 \\ x_4 \\ 0 \\ 0 \end{pmatrix} \rightarrow \begin{pmatrix} x_4 \\ 0 \\ 0 \\ 0 \end{pmatrix} \rightarrow \begin{pmatrix} 0 \\ 0 \\ 0 \\ 0 \end{pmatrix}$$

and $n_{min} = 4$. In the two parameter case, $(\tilde{\mathbf{A}} - \tilde{\mathbf{B}}\tilde{\mathbf{K}})$ will consist of two such nilpotent blocks along the diagonal, with zeros elsewhere, and $\mathbf{K}$ can be constructed such that each nilpotent block is 2×2. Thus, the above process takes place in each block, and $n_{min} = 2$ steps.

This convergence proceeds, however, at the expense of shuffling the coordinates of the state during the first $(n_{min} - 1)$ steps in the manner illustrated above, during which it is possible to move the trajectory outside of the region in which the linearization is valid. In this case the procedure fails. Thus, since two parameter control only requires one shuffling step while one parameter control requires three, the multiparameter case is more likely to successfully achieve control. For a typical (ρ^*, ϕ^*) pair in our numerical example, one parameter ρ control required an average of 197 attempts before successfully stabilizing the trajectory at the fixed point, while one parameter ϕ control required an average of 440 control attempts. These numbers may be contrasted with an average of only seven control attempts required in the case of two parameter control.

As mentioned above, when using several control parameters, the calculated perturbations may be within the allowed ranges for only a few of the components of $\mathbf{p}_n$. In this case, it is possible to apply only those perturbations and leave the other components unchanged. In the example above, this corresponds to setting either the upper or lower half of $(\tilde{\mathbf{A}} - \tilde{\mathbf{B}}\tilde{\mathbf{K}})$ to zero and nilpotent blocks. In our numerical experiments, no advantages were observed under this procedure. From a set of 10 000 trajectories begun at random initial conditions, 29.9% were stabilized as described above, but at the cost of increasing the overall average number of control attempts to 249.

Ideally, one would like to choose $(\mathbf{A} - \mathbf{B}\mathbf{K})$ such that no detrimental shuffling of coordinates occurs. Since chaotic transient trajectories approach the fixed point along the stable directions, at the time control is initiated, $\mathbf{x}$ will have small components in the unstable directions, but a large component in at least one stable direction. To avoid shuffling this large component into the other coordinates, one would like to move the trajectory directly onto the stable manifold, as originally proposed in Ref. [1]. This, however, can be problematic in the multiparameter case.

Even though $(\mathbf{A}-\mathbf{BK})$ can be constructed to have any desired eigenvalues, it may not be possible to simultaneously align its stable eigenvectors with those of $\mathbf{A}$. In this case, it may be best to use all zero eigenvalues.

In conclusion, we emphasize that the stabilization formalism presented here requires no global knowledge of the dynamics of the system, and thus represents an experimentally feasible way to reduce transient times and improve performance in the presence of noise.

This work was supported by the U.S. Department of Energy, Office of Scientific Computing. In addition, E.B. was supported by the National Physical Science Consortium under the sponsorship of Argonne National Laboratory. The numerical computations reported in this paper were supported in part by a grant from the W. M. Keck Foundation. The authors would like to thank E. Ott and J. A. Yorke for numerous helpful discussions.

APPENDIX

In this appendix we describe how to construct the matrix $\mathbf{K}$. For further details, the reader is referred to Ref. [12].

A controllable system is one for which a matrix $\mathbf{K}$ can be found such that $\mathbf{A}-\mathbf{BK}$ has any desired eigenvalues. This is possible if *rank* $\mathbf{C}=n$, where n is the number of dimensions of the state vector, and

$$\mathbf{C}=\left[\,\mathbf{B}\;:\;\mathbf{AB}\;:\;\mathbf{A}^2\mathbf{B}\;:\;\ldots\;:\;\mathbf{A}^{n-1}\mathbf{B}\,\right]$$

is the controllability matrix.

If only one control parameter is to be used, $\mathbf{K}$ is most easily obtained from Ackermann's formula

$$\mathbf{K}=\left[\,0\;\;0\;\cdots\;1\,\right]\mathbf{C}^{-1}\phi(\mathbf{A}),$$

where

$$\phi(\mathbf{A})=(\mathbf{A}-\mu_1\mathbf{I})(\mathbf{A}-\mu_2\mathbf{I})\cdots(\mathbf{A}-\mu_n\mathbf{I}),$$

in which the μ_i's are the desired eigenvalues.

In the multiparameter case, recall that the matrix $\mathbf{B}$ is $(n\times r)$. Denoting the columns of $\mathbf{B}$ by $\mathbf{B}_1,\mathbf{B}_2,\ldots,\mathbf{B}_r$, the controllability matrix can be written as

$$\mathbf{C}=\left[\,\mathbf{B}_1\;:\;\mathbf{B}_2\;:\;\ldots\;:\;\mathbf{B}_r\;:\;\mathbf{AB}_1\;:\;\mathbf{AB}_2\;:\;\ldots\;:\;\mathbf{AB}_r\;:\;\ldots\;:\;\mathbf{A}^{n-1}\mathbf{B}_1\;:\;\ldots\;:\;\mathbf{A}^{n-1}\mathbf{B}_r\,\right].$$

If the system is controllable, we can pick n linearly independent vectors from among the columns of $\mathbf{C}$. We test the columns as encountered from left to right, and then arrange the n columns found as follows to form the $(n\times n)$ matrix $\mathbf{M}$:

$$\mathbf{M}=\left[\,\mathbf{B}_1\;:\;\mathbf{AB}_1\;:\;\mathbf{A}^2\mathbf{B}_1\;:\;\ldots\;:\;\mathbf{A}^{n_1-1}\mathbf{B}_1\;:\;\mathbf{B}_2\;:\;\mathbf{A}^2\mathbf{B}_2\;:\;\ldots\;:\;\mathbf{A}^{n_r-1}\mathbf{B}_r\,\right].$$

This defines the numbers $n_1,n_2,\ldots,n_r$; notice that $\Sigma n_i=n$.

Calculating the inverse of this matrix, we define the η_i^{th} row vector of $\mathbf{M}^{-1}$ as $\mathbf{m}_i$, where $\eta_i=n_1+n_2+\cdots+n_i$ for $i=1,2,\ldots,r$. Further defining the $(n_i\times n)$ matrix

$$\mathbf{S}_i=\begin{bmatrix}\mathbf{m}_i\\ \mathbf{m}_i\mathbf{A}\\ \vdots\\ \mathbf{m}_i\mathbf{A}^{n_i-1}\end{bmatrix},$$

we then let

$$\mathbf{T}=\begin{bmatrix}\mathbf{S}_1\\ \mathbf{S}_2\\ \vdots\\ \mathbf{S}_r\end{bmatrix}^{-1}.$$

This matrix is $(n\times n)$, and as mentioned above, transforms the system to the controllable canonical form [12].

Thus, $\mathbf{A}$ is transformed to $\hat{\mathbf{A}}=\mathbf{T}^{-1}\mathbf{AT}$, which defines the numbers α_{ij} as follows:

$$\hat{\mathbf{A}}=\begin{pmatrix}
0 & 1 & 0 & \cdots & 0 & 0 & 0 & \cdots & 0 & 0 & \cdots & 0 & \cdots & 0\\
0 & 0 & 1 & \cdots & 0 & 0 & 0 & \cdots & 0 & 0 & \cdots & 0 & \cdots & 0\\
\vdots & \vdots & \vdots & \vdots & \vdots & \vdots & \cdots & \cdots & \vdots & \vdots & \vdots & \vdots & \vdots & \vdots\\
0 & 0 & 0 & \cdots & 0 & 0 & 0 & \cdots & 0 & 0 & \cdots & 0 & \cdots & 0\\
-\alpha_{11} & -\alpha_{12} & -\alpha_{13} & \cdots & -\alpha_{1n_1} & -\alpha_{1(n_1+1)} & -\alpha_{1(n_1+2)} & \cdots & -\alpha_{1(n_1+n_2)} & \cdots & \cdots & \cdots & \cdots & -\alpha_{1n}\\
0 & 0 & 0 & \cdots & 0 & 0 & 1 & \cdots & 0 & 0 & \cdots & 0 & \cdots & 0\\
\vdots & \vdots & \vdots & \vdots & \vdots & \vdots & \vdots & \vdots & \vdots & \vdots & \vdots & \vdots & \vdots & \vdots\\
-\alpha_{21} & -\alpha_{22} & -\alpha_{23} & \cdots & -\alpha_{2n_1} & -\alpha_{2(n_1+1)} & \cdots & \cdots & -\alpha_{2(n_1+n_2)} & \cdots & \cdots & \cdots & \cdots & -\alpha_{2n}\\
\vdots & \vdots & \vdots & \vdots & \vdots & \vdots & \vdots & \vdots & \vdots & \vdots & \vdots & \vdots & \vdots & \vdots\\
-\alpha_{n1} & -\alpha_{n2} & -\alpha_{n3} & \cdots & -\alpha_{nn_1} & -\alpha_{n(n_1+1)} & \cdots & \cdots & -\alpha_{n(n_1+n_2)} & \cdots & \cdots & \cdots & \cdots & -\alpha_{nn}
\end{pmatrix}.$$

Similarly, $\mathbf{B}$ is transformed to $\hat{\mathbf{B}} = \mathbf{T}^{-1}\mathbf{B}$:

$$\hat{\mathbf{B}} = \begin{pmatrix} 0 & 0 & 0 & 0 & 0 \\ \vdots & \vdots & \vdots & \vdots & \vdots \\ 0 & 0 & 0 & 0 & 0 \\ 1 & \beta_{12} & \cdots & \cdots & \beta_{1r} \\ 0 & 0 & 0 & 0 & 0 \\ \vdots & \vdots & \vdots & \vdots & \vdots \\ 0 & 0 & 0 & 0 & 0 \\ 0 & 1 & \beta_{23} & \cdots & \beta_{2r} \\ \vdots & \vdots & \vdots & \vdots & \vdots \\ \vdots & \vdots & \vdots & \vdots & \vdots \\ 0 & \cdots & \cdots & \cdots & 1 \end{pmatrix},$$

in which the the first block has n_1 rows, the second block has n_2 rows, etc. This defines the numbers β_{ij}.

If the desired eigenvalues of $(\mathbf{A} - \mathbf{BK})$ are all zeros, $\mathbf{K}$ is given by $\mathbf{K} = \mathbf{H}\Delta\mathbf{T}^{-1}$, where

$$\mathbf{H} = \begin{pmatrix} 1 & \beta_{12} & \beta_{13} & \cdots & \beta_{1r} \\ 0 & 1 & \beta_{23} & \cdots & \beta_{2r} \\ \vdots & \vdots & \vdots & \vdots & \vdots \\ 0 & \cdots & \cdots & \cdots & 1 \end{pmatrix}^{-1}$$

[note that $\mathbf{H}$ is an $(r \times r)$ matrix], and

$$\Delta = \begin{pmatrix} -\alpha_{11} & -\alpha_{12} & \cdots & -\alpha_{1n} \\ -\alpha_{21} & -\alpha_{22} & \cdots & -\alpha_{2n} \\ \vdots & \vdots & \vdots & \vdots \end{pmatrix}.$$

Δ is $(r \times n)$.

If instead of zeros the desired eigenvalues are $\mu_1, \ldots, \mu_n$, then the matrix Δ is determined by equating the coefficients of the characteristic equation of $(\hat{\mathbf{A}} - \hat{\mathbf{B}}\mathbf{H}\Delta - \lambda\mathbf{I})$ to those of the desired characteristic equation, namely, $(\mu_1 - \lambda)(\mu_2 - \lambda)\cdots(\mu_n - \lambda)$. The resulting equations are often fewer in number than nr, the number of entries in Δ, and thus Δ may not be unique.

[1] E. Ott, C. Grebogi, and J. A. Yorke, Phys. Rev. Lett. **64**, 1196 (1990).

[2] F. J. Romeiras, C. Grebogi, E. Ott, and W. P. Dayawansa, Physica D **58**, 165 (1992).

[3] W. L. Ditto, S. N. Rauseo, and M. L. Spano, Phys. Rev. Lett. **65**, 3211 (1990); B. Hubinger, R. Doerner, W. Martienssen, M. Herdering, and U. Dressler, Phys. Rev. E **50**, 932 (1994); J. Starrett and R. Tagg, Phys. Rev. Lett. **74**, 1974 (1994).

[4] R. Roy, T. W. Murphy, T. D. Maier, A. Gills, and E. R. Hunt, Phys. Rev. Lett. **68**, 1123 (1991); Z. Gills, C. Iwata, R. Roy, I. B. Schwartz, and I. Triandaf, *ibid.* **68**, 3169 (1992); S. Bielawski, M. Bouazaoui, D. Derozier, and P. Glorieux, Phys. Rev. A **47**, 3276 (1993); S. Bielawski, D. Derozier, and P. Glorieux, Phys. Rev. E **49**, R971 (1994); C. Reyl, L. Flepp, R. Badii, and E. Brun, *ibid.* **47**, 267 (1993); R. Meucci, W. Gadomski, M. Ciofini, and F. T. Arecchi, *ibid.* **49**, R2528 (1994).

[5] E. R. Hunt, Phys. Rev. Lett. **67**, 1953 (1991); G. A. Johnson and E. R. Hunt, Int. J. Bifurc. Chaos **3**, 1 (1993); D. J. Gauthier, D. W. Sukow, H. M. Concannon, and J. E. S. Socolar, Phys. Rev. E **50**, 2343 (1994).

[6] V. Petrov, V. Gaspar, J. Masare, and K. Showalter, Nature **361**, 240 (1993); V. Petrov, M. J. Crowley, and K. Showalter, Phys. Rev. Lett. **72**, 2955 (1994).

[7] A. Garfinkel, M. L. Spano, W. L. Ditto, and J. N. Weiss, Science **257**, 1230 (1992); S. J. Schiff, K. Jerger, D. H. Duong, T. Chang, M. L. Spano, and W. L. Ditto, Nature **370**, 615 (1994).

[8] E. Barreto, E. J. Kostelich, C. Grebogi, E. Ott, and J. A. Yorke, Phys. Rev. E **51**, 4169 (1995).

[9] T. Shinbrot, E. Ott, C. Grebogi, and J. A. Yorke, Phys. Rev. Lett. **65**, 3215 (1990); Phys. Lett. A **45**, 4165 (1992); T. Shinbrot *et al.*, Phys. Rev. Lett. **68**, 2863 (1992); E. Bollt and J. D. Meiss, Physica D **81**, 280 (1995).

[10] J. Warncke, M. Bauer, and W. Martienssen, Europhys. Lett. **25**, 323 (1994).

[11] E. J. Kostelich, C. Grebogi, E. Ott, and J. A. Yorke, Physica D **25**, 347 (1987); Phys. Lett. A **118**, 448 (1986); **120**, 497(E) (1987).

[12] K. Ogata, *Discrete-Time Control Systems* (Prentice Hall, Englewood Cliffs, NJ, 1987).